Superalloys 2004
Edited by K.A. Green, T.M. Pollock, H. Harada, T.E. Howson, R.C. Reed, J.J. Schirra, and S. Walston
TMS (The Minerals, Metals & Materials Society), 2004

ATOMIC PARTITIONING OF RUTHENIUM IN NI-BASED SUPERALLOYS

S. Tin[1], A.C. Yeh[1], A.P. Ofori[1], R.C. Reed[2], S.S. Babu[3] and M.K. Miller[3]
[1]Dept of Materials Science & Metallurgy,
University of Cambridge, Pembroke Street, Cambridge CB2 3QZ, UK
[2]Dept of Metals and Materials Engineering,
The University of British Columbia, 309-6350 Stores Road, Vancouver V6T 1Z4, Canada
[3]Metals and Ceramics Division, Oak Ridge National Laboratory, PO Box 2008, TN 37831-6136, USA

Keywords: Single crystal, Partitioning, Ruthenium, Atom Probe and ALCHEMI

Abstract

The elemental partitioning characteristics of Ru additions within the microstructure of high refractory content Ni-base single crystal superalloys have been investigated using atom probe tomography (APT). Although detailed microanalysis revealed some dissolution of Ru within the ordered intermetallic γ′ precipitates, Ru was observed to preferentially partition to the disordered γ matrix. The partitioning characteristics of two nominally similar alloys with and without Ru were studied as part of this investigation. Analyses indicate that no significant changes in the partitioning characteristics of the constituent elements could be attributed to the presence of Ru for this particular set of alloys. The preferential site occupancy of Ru within the $L1_2$ lattice was also statistically quantified using ALCHEMI (atomic site location by channelling enhanced microanalysis). Interestingly, Ru exhibited a tendency to substitute for Al and occupy the corner sites in the γ′ structure.

Introduction

Single crystal nickel-base superalloys have been extensively engineered to provide an unparalleled combination of structural properties at elevated temperature. Coupled with an improved understanding of the mechanisms governing high temperature deformation, improvements in processing and the development of advanced alloys enable these structural metallic materials to operate at temperatures (T_H=85-90%) approaching their melting point. Refractory additions, such as rhenium, have played a key role in improving the high temperature properties of this class of material. However, additions of platinum group metals (PGMs) and ruthenium in particular have emerged as potential alloying elements that may further enhance the structural properties of single crystal Ni-base superalloys and extend their temperature capability[1, 2]. At this time, the beneficial effects are not well understood, although it has been postulated that ruthenium alters the partitioning of elements between the γ and γ′ phases[3]. Furthermore, it has been suggested that ruthenium has the effect of reducing the susceptibility to the precipitation of topologically close-packed (TCP) phases, for reasons that are yet to be elucidated. It is clear that more work is required to identify the roles of ruthenium in superalloy metallurgy.

In this paper, atom probe tomography (APT) analysis was used to carry out very high-resolution microanalysis of the elemental partitioning characteristics in two experimental alloys, of the type used for turbine blade aerofoils. The compositions of the two alloys are similar, but the second is alloyed with ruthenium. The atom probe is particularly well suited for the determination of elemental partitioning in superalloy systems[4-8]. The work was motivated particularly by the desire to provide basic understanding of the ruthenium effect, to identify any synergistic effects induced on the partitioning of the various elements between the γ and γ′ phases and to help identify the factors influencing its role in promoting alloy stability. Furthermore, ALCHEMI techniques were also utilized to investigate the atomic site partitioning characteristics of Ru within the ordered intermetallic γ′ phase.

Experimental Methods

The atomic partitioning of Ru in Ni-base superalloys was studied using a tertiary Ni-Al-Ru alloy and two experimental single crystal alloys designated RR2100 and RR2101, Table I. Polycrystalline samples of the ternary Ni-Al-Ru alloy were vacuum arc melted from high purity elemental bar stock and homogenized at 1365˚C for eight hours to minimize residual segregation. The single crystal alloy, RR2100, is an experimental superalloy with refractory alloying levels, Re content of 6.4 wt%, 9 wt% of W, 5.5 wt% of Ta, similar to those present in other advanced single crystal superalloys. With the exception of a 2 wt% Ru addition which was substituted directly for Ni, alloy RR2101 is nominally similar to RR2100. The single crystal alloys were vacuum induction melted by Ross & Catherall Ltd, Sheffield, UK and fabricated by Rolls-Royce plc using standard investment casting procedures. Single crystals were solution heat treated using a long, ramped cycle rising in steps to 1365˚C, at which temperature the material was held for 20 h. A primary age of 5 h at 1140˚C was also applied.

High-resolution characterization of chemical partitioning between the γ and γ′ phases, was carried out at the facilities of Oak Ridge National Laboratory using an energy-compensated optical position-sensitive atom probe. For this study, characterization of the single crystals with the atom probe was limited to as-received specimens. Atom probe tomography (APT) composition analyses were performed with a specimen temperature of 60 K, a pulse fraction of 20% and a pulse repetition rate of 1.5kHz. For each alloy, at least three specimens were analyzed.

Compositions of the experimental single crystal alloys after the heat treatment were verified using X-ray fluorescence (XRF). Bulk electrolytic extraction of γ′ precipitates from the single crystals was performed using a solution of 5% nitric and 2% perchloric acid in water and a current density of 0.1 A/cm^2. The extracted precipitates were sent to IncoTest, Hereford, UK for wet

Table I: Nominal Composition of the Experimental Ni-base superalloys (wt% and [at%])

Alloy	Co	Cr	W	Re	Ru	Al	Ta	Hf	Ni
RR2100	12 [12.8]	2.5 [3.0]	9.0 [3.1]	6.4 [2.2]	0	6 [14.0]	5.5 [1.9]	0.15 [0.06]	Balance
RR2101	12 [13.0]	2.5 [3.0]	9.0 [3.1]	6.4 [2.2]	2.0 [1.3]	6 [14.2]	5.5 [1.9]	0.15 [0.06]	Balance
Ni-Al-Ru	-	-	-	-	5.7 [3.0]	9.4 [18.9]	0	0	Balance

chemical analysis. TEM specimens were prepared by mechanically grinding thin discs of sample material followed by electrolytic thinning. A twin-jet polisher along with a solution of 10 vol% perchloric acid in ethanol at approximately -5°C was used for this latter stage.

To perform statistical ALCHEMI, a Philips FEGTEM CM300 TEM was used in rocking beam mode. X-ray spectra were collected as a function of position, as a 200kV, 50nm electron beam was scanned about a 95×75 mrad surface centered on a low-index major zone axis of a γ′ precipitate. The way in which similar atomic sites line up when Ni_3Al is viewed along the <100> and <111> zone axes identify these orientations as the most suitable for ALCHEMI. Spectra were recorded over an 80×60 step array, with an acquisition time of 1.5s per spectrum and a count rate of about 10,000 counts per second. Once acquisition was completed the 4800 spectra were processed to give background-subtracted elemental maps for Ni, Al and any other alloying additions. Since statistical ALCHEMI relies on the premise that the partitioning of a doping species correlates with the extent of superposition required to form the dopant map from the host site maps, application of χ^2-minimisation was used to identify the atomic site partitioning values and to provide a measure of confidence in the fit of the model to the experimental data.

Results

Microstructures of the single crystal alloys and the ternary Ni-Al-Ru alloy are presented in Figure 1. After the solution heat treatment, the microstructures of all three alloys consisted of large fractions of coherent cuboidal shaped γ′ precipitates contained within a γ matrix. No noticeable differences in precipitate size, morphology and volume fraction were observed between alloy RR2100 and RR2101. Compared to the multicomponent single crystal alloys, the γ′ precipitates in the ternary Ni-Al-Ru alloy were noticeably more spherical.

The APT datasets were analyzed using statistical methods and involved the visualization of the atomic positions using 3D rendering software, Figure 2. With the exception of the presence of Ru in alloy RR2101, visual analysis of the 3D plots revealed no noticeable differences in elemental partitioning behavior between the two single crystal alloys. Due to the size and volume fraction of the γ′ precipitates, (~75% and ~500nm, respectively) the continuous γ channels between the precipitates typically measured well below 100nm. Coupled with the small volumes (15nm x 15nm x 50nm) analyzed in the atom probe, the large dimensional differences between the microstructural features prevented consistent delineation of $\gamma - \gamma'$ interfaces during analyses. Hence, multiple specimens were analyzed during the course of this investigation.

Good general agreement was observed when the compositional information from the APT, XRF and wet chemical analyses were compared, Table II. Using the APT data, compositions of the phases (atom fraction) were plotted as functions of $C_i^n - C_i^\gamma$ *vs* $C_i^{\gamma'} - C_i^\gamma$ for *i*=Al, Ta, Re, Ru, etc. to calculate the overall fraction of γ′ present in the alloy. C_i^n, C_i^γ *and* $C_i^{\gamma'}$ correspond to the level of element, *i,* contained within the bulk, γ and γ′ phases, respectively. Values of C_i^γ and $C_i^{\gamma'}$ were averaged from multiple atom probe analyses and values of C_i^n from the known bulk alloy composition. The mass balance assessment[7] for each of the alloys is presented in Figure 3. With the slope of the best fit line corresponding to the volume fraction of γ′ present within the alloy, the addition of Ru to RR2101 did not appear to significantly alter the fraction of the γ′ phase – computed values were 77.3% for RR2100 and 77.6% for RR2101 respectively.

When present, compositional differences were used to identify the location of the $\gamma - \gamma'$ interfaces. Exhibiting a $L1_2$ structure, the intermetallic γ′ phases are highly enriched with Al and Ta, while the solid solution strengthened FCC matrix contains characteristically elevated levels of Co, Cr and Re. The averaged $\gamma - \gamma'$ partitioning coefficients determined from the data are listed in Table 2, with standard deviations quoted based upon the counting statistics. As an alloying addition in RR2101, Ru was observed to partition preferentially to the γ phase in a manner similar to Re, Cr and Co. Comparison of the results from RR2100 and RR2101 suggest that the influence of Ru on the characteristic partitioning behavior of the other constituent elements was negligible, Table III. Despite the presence of Ru in RR2101, the degree of alloying measured within the respective $\gamma - \gamma'$ phases was nominally identical to RR2100. Detailed characterization of the $\gamma - \gamma'$ interfaces was also performed and the composition profiles across them were distinct, Figure 4. Interfacial segregation of refractory elements with low levels of solubility in the γ′ phase could not be statistically quantified in the solutioned and aged specimens.

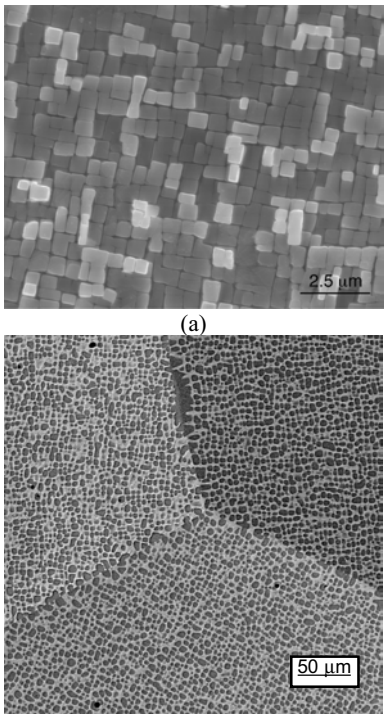

Figure 1: Microstructures of the single crystal Ni-base superalloy (a) RR2100 and the (b) ternary Ni-18.9-3Ru (at%) alloy.

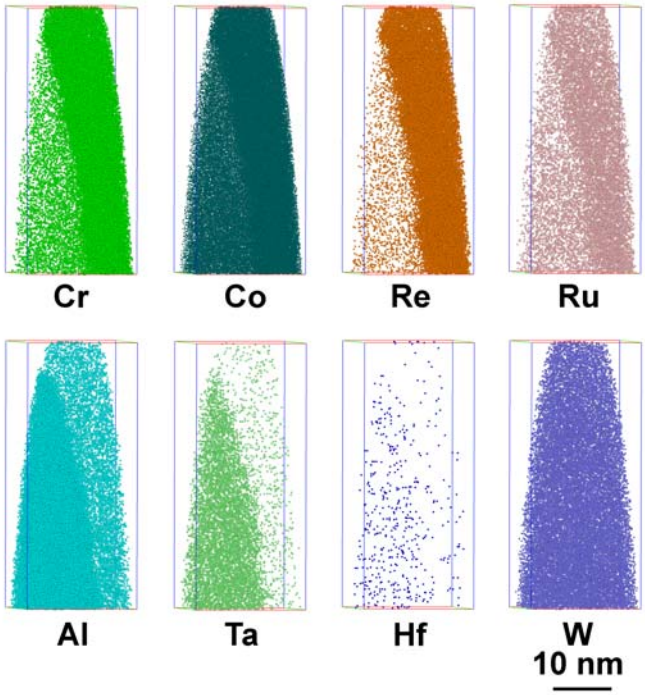

Figure 2: Three Dimensional Elemental Reconstruction of the γ – γ′ Interface for RR2101 with 2 wt.% Ru.

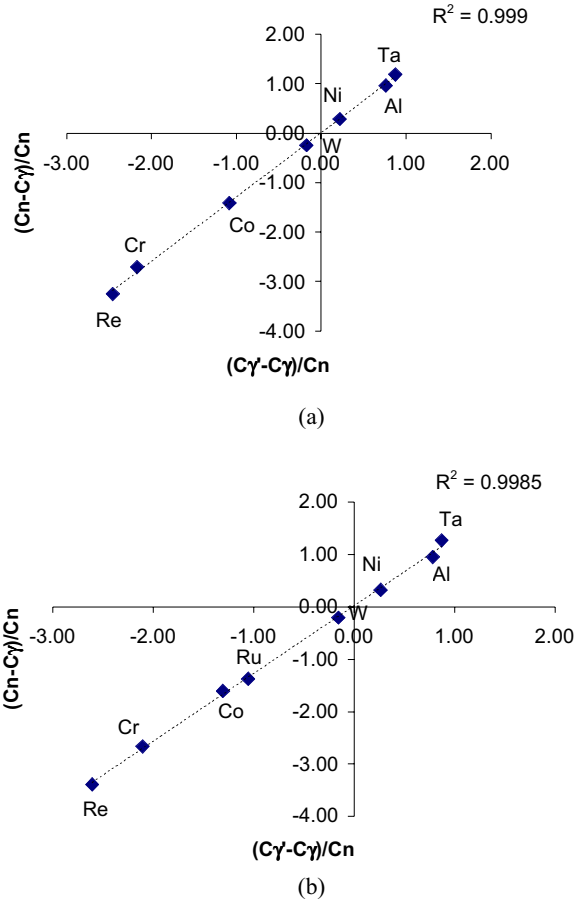

Figure 3: Plots of the normalized compositional distribution in the γ – γ′ phases for (a) RR2100 without Ru and (b) RR2101 with 2 wt.% Ru.

Site occupancy of Ru within the γ′ phase was also investigated with the atom probe. Statistical analyses indicate that Ru exhibits a slight preference for the Al corner sites within the $L1_2$ structure. Based on the APT data from RR2101, ~52% of the Ru atoms were estimated to reside along the crystallographic planes containing ordered sites for Ni and Al.

ALCHEMI analysis was performed to further verify the atomic site occupancy of Ru within the γ′ phase. Initial trials on high refractory content Ni-base superalloys revealed that the Ni and Al host site maps were influenced by the degree of alloying and were difficult to quantify statistically in complex multicomponent alloys. Computational simulations also revealed that the degree of alloying in γ′ could potentially limit the resolution of the ALCHEMI analyses. In particular, atomic delocalization and X-ray absorption were shown to strongly attenuate the differential responses on which ALCHEMI hinges.

Difficulties in quantifying the atomic site partitioning of Ru in γ′ were overcome by utilizing a simplified ternary Ni-18.9Al-3.0Ru (at%) alloy in the ALCHEMI analyses. Initially, a rocking beam scan on a binary Ni-18.9Al (at%) alloy was performed at room temperature to confirm adequate site discrimination between Ni and Al. As the X-ray channelling patterns are specific to atomic

Table II: Compositional Analyses of the Various Phases Present in RR2100 and RR2101(at%)

Alloy	Phase/Technique	Ni	Al	Ta	W	Re	Co	Cr	Ru
RR2100(γ')	γ'/APT	67.05	16.89	2.51	2.86	0.44	8.57	1.38	-
RR2101(γ')	γ'/APT	66.09	16.55	2.71	2.96	0.47	8.79	1.34	0.88
RR2100(γ)	γ /APT	49.11	3.09	0.24	3.62	7.50	26.74	9.51	-
RR2101(γ)	γ /APT	46.02	3.08	0.25	3.60	7.89	26.65	9.50	2.90
RR2100 (γ')	Extracted γ'/wet chem.	65.32	16.74	2.65	4.30	0.55	8.70	1.67	-
RR2101 (γ')	Extracted γ'/wet chem.	62.81	16.25	3.08	4.69	0.58	8.80	2.13	1.58
RR2100	Bulk/XRF	62.82	14.20	1.93	3.10	2.16	12.83	2.96	-
RR2101	Bulk/XRF	61.43	13.97	1.94	3.14	2.18	13.01	3.08	1.25

Table III: Elemental Partition Coefficients for RR2100 and RR2101

Alloy	Ni	Al	Ta	W	Re	Co	Cr	Ru
RR2100 γ/γ'	0.73	0.18	0.10	1.27	17.01	3.12	6.88	-
RR2101 γ/γ'	0.70	0.19	0.09	1.22	16.94	3.03	7.10	3.31

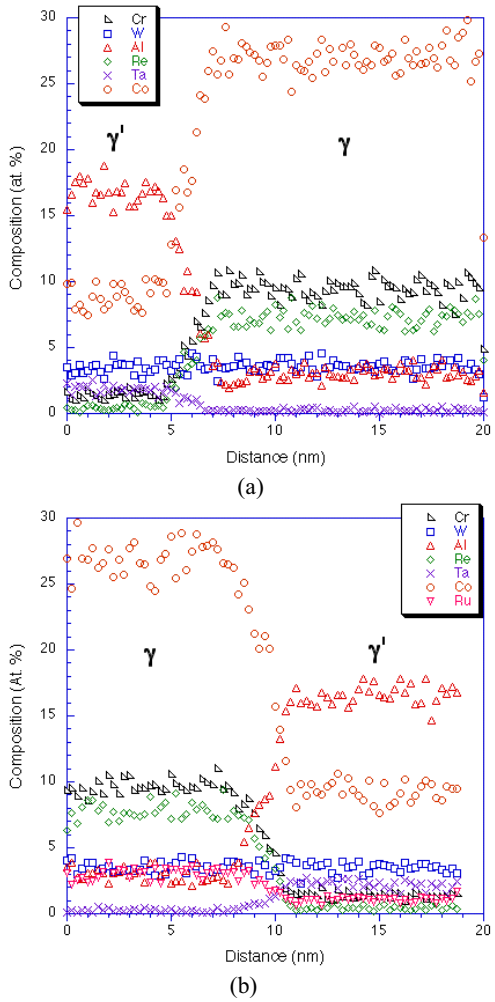

Figure 4: Elemental profile at the γ – γ′ interface for (a) RR2100 without Ru and (b) RR2101 with 2 wt.% Ru.

location, analysis of the patterns enables the Ni and Al sites within the ordered $L1_2$ crystal lattice to be distinguished. The ternary Ni-18.9Al-3.0Ru (at%) alloy was also analyzed in the same manner. The electron channelling pattern along with the X-ray channelling pattern for the ternary alloy can be seen in Figure 5. Characteristic X-ray maps corresponding to each of the constituent elements, Ni, Al and Ru, were clearly identified. Site locations of Ru were determined via linear superposition of the Ni and Al X-ray maps. Since the superimposed Ni/Ru pattern was divergent while the Al/Ru pattern exhibited excellent conformity, the ALCHEMI analysis indicates that Ru tends to partition preferentially to the Al sites in the $L1_2$ crystal lattice. Statistical values for relative site partitioning, f_{xi}, were calculated using a computational program based on matching of the X-ray maps.

Preference ratios, $k_{Ni/Al}$, were then evaluated by considering the 1:3 ratio of Al sites to Ni sites:

$$k_{Ni/Al} = \frac{f_{PGM,Ni}}{3.f_{PGM,Al}}$$

To ensure statistical validity of the analysis, ALCHEMI was repeated several times on the Ni-18.9Al-3Ru (at%) specimens using different precipitates, orientations and scanning conditions, Table IV. In all cases the site distribution ratios were found to be reasonably similar and highly reproducible.

Discussion

Although a number of recent studies have demonstrated that additions of Ru to high refractory content Ni-base superalloys can be effectively utilized to enhance high temperature phase stability and creep resistance[9, 10], the effects of Ru on the mechanisms contributing to the degradation of structural properties at high temperature are not well understood. Results from this investigation assist in the fundamental understanding and clearly reveal the characteristic partitioning tendencies of Ru additions in high refractory content single crystal Ni-base superalloys. When present in relatively low levels (~2 wt%) substantially higher levels of Ru were measured in the γ phase, Figure 4 and Table II. However, compared to some of the other constituent elements that also segregate strongly to the γ phase, Re, Co and Cr, the degree of Ru partitioning was relatively low as some dissolution of Ru occurred in the γ′ phase.

The formation of topologically-close-packed (TCP) phases in Ni-base superalloys has generally been attributed to the supersaturation of high melting point refractory elements (Re, W, Mo and Cr) within the disordered γ phase[11-15]. As the levels of

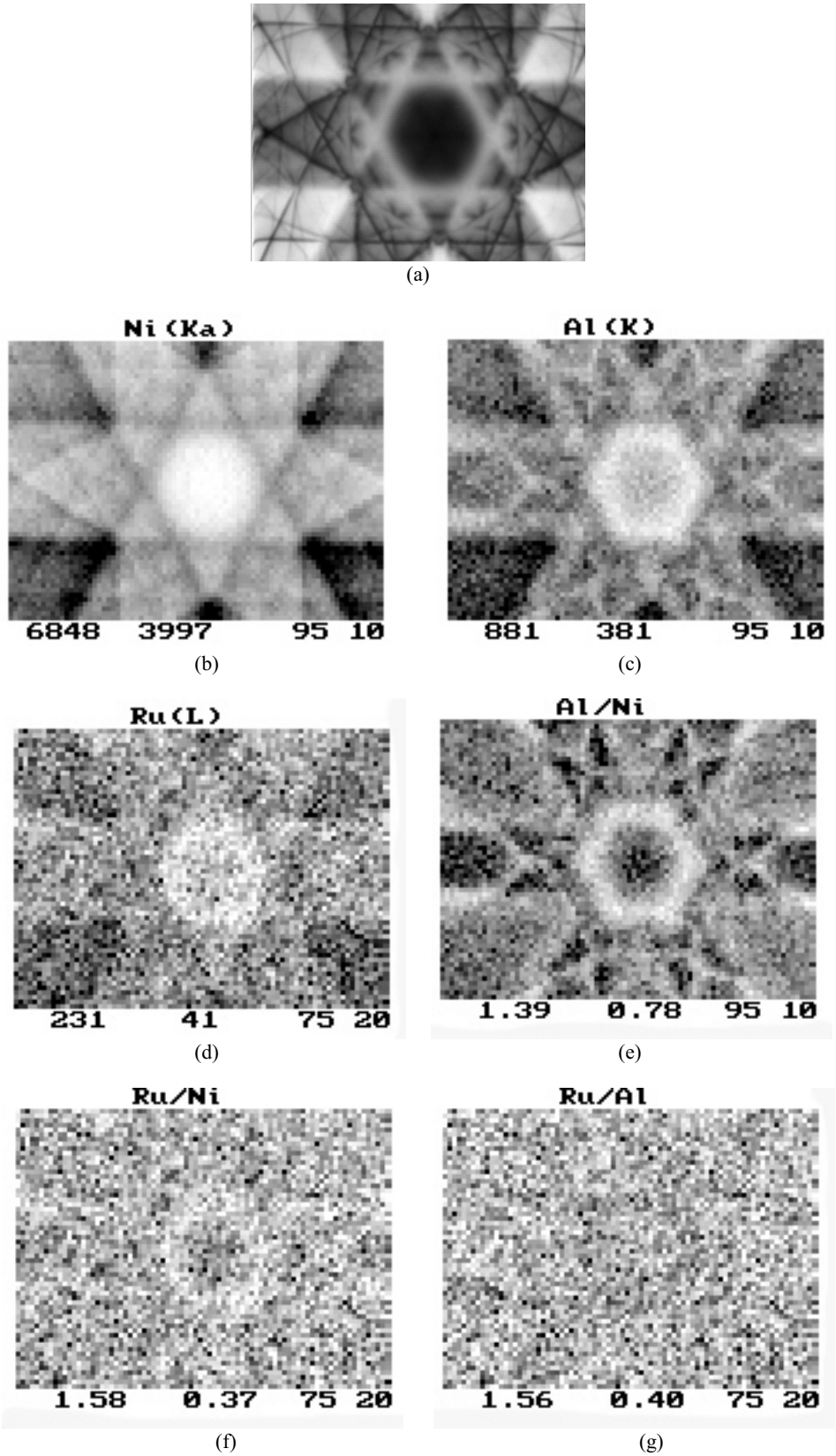

Figure 5: ALCHEMI electron channeling and X-ray patterns corresponding to Ni-18.9Al-3.0Ru (at%) revealing the atomic site partitioning tendencies of Ru in the γ' phase. (a) Electron channeling map, (b) to (d) elemental X-ray maps and (e) to (g) superposition of X-ray maps.

Table IV: Summary of the ALCHEMI Analyses on Ni-18.9Al-3.0Ru (at%)

Alloy	Zone	γ′ comp (at%)			Pixels (i.e. X-ray spectra)	Average cps	Relative partitioning of Ru (%)			Ni preference ratio	
		Ni	Al	Ru			$f_{Ru,Ni}$	error (+/-)	χ^2_R	$k_{Ni/Al}$	error (+/-)
NiAlRu	<100>	74.0	24.0	2.0	40x29	55,000	36.9	1.1	1.01	0.20	0.01
	<111>	74.0	24.0	2.0	80x60	13,500	44.4	1.6	0.98	0.27	0.02
	<111>	75.0	23.0	2.0	80x60	22,000	42.4	1.4	1.01	0.25	0.01

these refractory alloying additions were increased to enhance creep properties, the limited degree of refractory element solubility within the γ′ phase increased the susceptibility of these alloys to TCP formation. Initial studies attributed the beneficial effects of Ru-bearing Ni-base superalloys to a change in partitioning behavior. As increased levels of refractory element solubility were observed in the γ′ phase of experimental alloys containing Ru, the resulting change in compositional partitioning resulted in a smaller degree of refractory element supersaturation in the γ phase and enabled the Ru-bearing alloys to be more resistant to the formation of TCP phases[3]. In the present study, however, no significant changes in partitioning were observed between nominally identical alloys with and without additions of Ru, Figure 4 and Table III. Despite the presence of Ru in both the γ and γ′ phases of RR2101, the constituent elements in the respective phases do not appear to become displaced as the partition coefficients for RR2100 and RR2101 remain essentially unchanged.

Differences in the high temperature phase stability of these alloys have been previously reported[9]. With nearly identical levels of refractory element supersaturation in the γ phase, the Ru-bearing alloy exhibited a much higher degree of microstructural stability during static isothermal exposures over temperatures of 1000˚C to 1180˚C. Detailed analysis identified the TCP phases present in both RR2100 and RR2101 to be predominately P and σ phases. Interestingly, when present within the microstructure of the Ru-containing alloy, Ru was found to be insoluble in the P and σ-phase TCP precipitates. With an extended incubation period prior to the onset of TCP phase formation as well as a sluggish growth rate, the preferential presence of Ru in the γ phase appears to inhibit both the nucleation and growth of these undesirable phases.

The characteristic partitioning behavior of Ru may also influence the response of the alloy during creep deformation. Similar to the other constituent alloying elements with a hexagonal close packed (HCP) structure (Re and Co) preferential partitioning of Ru to the γ phase is likely to lower the stacking fault energy and influence the mobility of dislocations during the initial stages of creep.

Since some dissolution of Ru occurred within the ordered γ′ phase, atomic site location partitioning of Ru was also investigated. As the level of alloying in multicomponent alloys increases, solid solution strengthening of the intermetallic γ′ also occurs. Since properties, such as the anti-phase boundary (APB) energy and lattice parameter, can potentially be influenced by the site occupancy of the solute elements, the ability to identify the characteristic sites associated with each solute species may enable further optimization of the alloy. Such investigations are currently in progress. Elements, such as Ta, Hf, Ti and Nb, that promote the formation of γ′ tend to substitute directly for Al and occupy the corner sites within the $L1_2$ structure. Co and Cr additions tend to substitute directly for Ni in the γ′ phase. With atomic radii that are intermediate between Ni and Al, other refractory alloying additions (W, Re and Mo) tend to occupy both Ni and Al sites with a slight preference for the Al sites. Consistent with the ALCHEMI analyses on the ternary Ni-18.9-3Ru (at%) alloy, statistical analyses of the RR2101 using the atom probe data indicated Ru exhibited a slight preference for the Al site in the $L1_2$ structure. Interestingly, Ru was identified to be the only element within the platinum-group metal family (Ir, Pt, Rh, Pd and Ru) to partition preferentially onto the Al sites[16]. These trends were expected since Fe, which is from the same group of elements as Ru on the periodic table, also showed a tendency to occupy the Al sites in the γ′ phase and partition preferentially to the γ in IN718[17].

To summarize, this study clearly reveals both the characteristic phase partitioning and atomic site preference of Ru for this particular set of experimental single crystal Ni-base superalloys. Other than the enrichment of the γ by Ru at the expense of Ni, the concentrations of the other solute species in that phase are not altered substantially. As Ru is present in both the γ and γ′ phases, understanding the fundamental elemental interactions and how various properties are affected by the presence of Ru becomes critical. Results presented in this study may have significant implications on how Ru additions can potentially be utilized to extend the temperature capability of advanced single crystal Ni-base superalloys.

Conclusions

Atom probe tomography was used to characterize the elemental partitioning characteristics of two single crystal superalloys, one of which is doped with ruthenium. In support of the APT analyses, ALCHEMI was performed to further quantify the atomic site partitioning characteristics of Ru in two phase γ – γ′ alloys. The following conclusions could be drawn from this work:

1. Ru was found to partition preferentially to the γ matrix, with a partitioning coeffcient of 3.3.
2. The other alloying additions partitioned as expected, *i.e.* Cr,

Re & Co to γ and Ta & Hf to γ'. Little tendency to partition was displayed by W. The effect of Ru on partitioning of the other solutes was not substantial, but there was some evidence that it caused Ni and Al to leave the γ' phase, with these elements being replaced with W, Ta and Re.

3. The fraction of the γ phase was not altered significantly by the addition of Ru. Despite this fact, stability with respect to TCP precipitation was very much improved.

4. When present in the γ' phase, Ru tends to preferentially occupy the Al corner sites in the $L1_2$ lattice.

Acknowledgements

Research at the Oak Ridge National Laboratory SHaRE User Center was sponsored by the Division of Materials Sciences and Engineering, U.S. Department of Energy, under contract DE-AC05-00OR22725 with UT-Battelle, LLC.

References

1. Murakumi, H., T. Honma, Y. Koizumi, and H. Harada, *Superalloys 2000*. Warrendale, PA, TMS. p. 747-756.
2. Caron, P., *Superalloys 2000*, Warrendale, PA, TMS. p. 737-746.
3. O'Hara, K., W.S. Walston, E.W. Ross, and R. Darolia, in *US Patent* #5482789, (1996).
4. Yoon, K.E., D. Isheim, R.D. Noebe, and D.N. Seidman, Interface Science, 2001. **9**. p. 249-255.
5. Warren, P.J., A. Cerezo, and G.D.W. Smith, Materials Science and Engineering, 1998. **250A**. p. 88-92.
6. Blavette, D., E. Cadel, and B. Deconihout, Materials Characterization, 2000. **44**. p. 133-157.
7. Blavette, D., P. Caron, and T. Khan. in *Superalloys 1988*. Warrendale, PA, TMS. p. 305-314.
8. Rusing, J., N. Wanderka, U. Czubayko, V. Naundif, D. Mukherji, and J. Rosler, Scripta Mat., 2002. **46**. p. 235-240.
9. Yeh, A.C. and S. Tin. in *Parsons 2003*. IOM. p. 673-686.
10. Zhang, J.X., T. Murakamo, Y. Koizumi, T. Kobayashi, and H. Harada, Acta. Materialia, 2003. **51**. p. 5073-5081.
11. Rae, C.M.F., M.S.A. Karunaratne, C.J. Small, R.W. Broomfield, C.N. Jones, and R.C. Reed. in *Superalloys 2000*. Warrendale, PA, TMS. p. 767-776.
12. Wlodek, S.T. in *Long Term Stability of High Temperature Materials*. 1999. Warrendale, PA, TMS. p. 1-38.
13. Wlodek, S.T., Trans. ASM, 1964. **57**. p. 110-119.
14. Ross, E.W., J. Met., 1967. p. 12-14.
15. Darolia, R., D.F. Lahrman, and R.D. Field. in *Superalloys 1988*. Warrendale, PA, TMS. p. 255-264.
16. Ofori, A.P., S. Tin, C.J. Humphreys, and C.N. Jones. in *Superalloys 2004*. Warrendale, PA, TMS.
17. Miller, M.K and S.S. Babu, in Superalloys 718, 625, 706 and Derivatives 2001, Warrendale, PA, TMS, p. 357-365.